



## Description and biological observations on a new species of deepwater symphurine tonguefish (Pleuronectiformes: Cynoglossidae: *Symphurus*) collected at Volcano–19, Tonga Arc, West Pacific Ocean

THOMAS A. MUNROE<sup>1,3</sup>, JENNIFER TYLER<sup>2</sup> & VERENA TUNNICLIFFE<sup>2</sup>

<sup>1</sup>National Systematics Laboratory, National Marine Fisheries Service, NOAA, Smithsonian Institution, Post Office Box 37012, National Museum of Natural History, WC–57, MRC–153, Washington, DC 20013–7012, USA. E-mail: munroet@si.edu

<sup>2</sup>Department of Biology, University of Victoria, PO Box 3080, Victoria, British Columbia, Canada V8W 3N5. E-mail: verenat@uvic.ca; jentylert24@gmail.com

<sup>3</sup>Corresponding author. E-mail: munroet@si.edu

### Abstract

*Symphurus maculopinnis* n. sp., described on a single specimen (USNM 398820; 84.4 mm SL), was collected by a remotely operated vehicle (ROV) exploring a hydrothermal vent area located at 561 m on Volcano–19, Tonga Arc, West Pacific (24°48.439' S, 177°0.009' W). This new species is distinctive and readily diagnosed from congeners by the following combination of characters: 1–2–2–1 pattern of interdigitation of dorsal proximal pterygiophores and neural spines (ID pattern), 14 caudal-fin rays, 3+6 abdominal vertebrae, 49 total vertebrae, 89 scales in a longitudinal row, 92 dorsal-fin rays, 77 anal-fin rays, blunt squarish snout, thick blind-side lips with conspicuous plicae, and conspicuous ocellated (sometimes partially) spots on posterior dorsal and anal fins. Among *Symphurus*, only *S. ocellatus* von Bonde, collected at deepwater locations off East Africa, features a similar ID pattern, 14 caudal-fin rays and spots on the posterior dorsal and anal fins. *Symphurus maculopinnis* differs distinctly from *S. ocellatus* in its lower and non-overlapping meristic features (49 vs. 54–56 total vertebrae; 92 vs. 97–103 dorsal-fin rays; and 77 vs. 85–89 anal-fin rays), its squarish (vs. pointed) snout, and thick, plicated blind-side lower lip (vs. thin, non-plicated blind-side lower lip). Additional specimens (N= 56) of *S. maculopinnis* observed and filmed *in situ* near active venting sites located between ca. 433–561 m on Volcano–19 provide the basis for behavioral and ecological information recorded for the species. Videotapes reveal one individual of *S. maculopinnis* featuring reversed (dextral) asymmetry from that typical (sinistral) for members of the Cynoglossidae. Specimens with reversed asymmetry are relatively rare in this family and this *S. maculopinnis* represents only the second known reversed individual among the approximately 42 species of deep-sea (>200 m) *Symphurus*.

**Key words:** taxonomy, deep-sea flatfish, tongue sole, hydrothermal vents, volcanic arcs, seamounts, reversed asymmetry, species description, ocelli

### Introduction

Exploratory expeditions along the Tonga and Kermadec Volcanic Arcs investigated various features of submarine volcanoes, hydrothermal vents and their associated faunas (e.g. Stoffers *et al.* 2006). Of particular interest during these expeditions was the discovery of symphurine tonguefishes associated with deepwater hydrothermal vents and other habitats on these undersea volcanoes (Tunnicliffe *et al.* 2010). One undescribed tonguefish species, Species B, observed on Volcano–19 in the Tonga Arc, was conspicuous in the possession of a single pigmented spot on both the posterior dorsal and anal fins. This pigmentation feature is rare among species of Indo–West Pacific *Symphurus* (Munroe unpubl. data), with only *S. ocellatus* von Bonde collected from deep waters in the western Indian Ocean having such spots on its dorsal and anal fins.

A single specimen (now the holotype) of this undescribed species, collected at 561 m on Volcano–19 during a dive conducted by the ROV *ROPOS*, provides the basis for formal description of this species. Details of the expeditions including physico-chemical data of habitats where this specimen was collected and where other specimens of this species were observed, as well as ecological and behavioral observations for the new species, were provided in Tunnicliffe *et al.* (2010).

## Material and methods

The holotype (USNM 398820) is deposited in the fish collection of the United States National Museum. Description of this species is based on counts and measurements from the holotype, with features of live pigmentation provided by a photograph of the holotype prior to collection (Fig. 1) and photographs of additional specimens filmed *in situ* on Volcano-19 from a remotely operated vehicle (ROV). Comparative materials for other Indo-Pacific species of *Symphurus* are detailed in Munroe (1992), Krabbenhoft and Munroe (2003), Munroe (2006), Munroe and Hashimoto (2008), and Lee *et al.* (2009a).



**FIGURE 1.** Holotype of *Symphurus maculopinnis*, n. sp. (now USNM 398820), photographed *in situ* just prior to collection by ROV *ROPOS* at 561 m on Volcano-19, Tonga Arc, West Pacific. Manipulator is holding a scoop net.

Methods for counts and measurements and general terminology for systematics of tonguefishes follow those of Munroe (1998). Terminology for interdigitation patterns of proximal dorsal pterygiophores and neural spines (ID pattern) follow that of Munroe (1992). ID patterns, fin ray and vertebral counts were made from radiographs.

Standard length (SL) and head length (HL) are used throughout. Measurements were made to the nearest 0.1 mm using either dial calipers or a dissecting stereo microscope fitted with a calibrated ocular micrometer. Morphometric features are expressed either as measurements in percentages of standard length, or percentages of head length. Pigmentation of alcohol-preserved fish is based on the holotype, which was originally fixed in 95% ethanol and then transferred and stored in 75% ethanol. Habitat descriptions and behavioral observations are based on fishes videotaped *in situ* and reported on by Tunnicliffe *et al.* (2010), with additional observations made from two fish appearing in a short video provided from the ROV *ROPOS* (Cruise Chief Scientist Dr. Ulrich Schwarz-Scham-

pera) and edited by Jonathan Rose (University of Victoria; video available at <http://ocean.si.edu/ocean-videos/tonguefish-underwater-volcano-19>). Size at maturity was determined from the stage of ovarian development in the female holotype following criteria outlined in Munroe (1998).

***Symphurus maculopinnis*, new species**

Figures 1–7; Table 1

*Symphurus* species B. Tunncliffe *et al.* 2010:4 (species recognition; bathymetric and ecological notes; genetic sequence data; distribution, abundance; color photographs).

**Holotype.** USNM 398820, female, 84.4 mm SL, collected on Volcano-19 near Marker 40, Tonga Arc (24°48.439'S, 177°0.009'W), West Pacific Ocean, 561 m, collected with hand-held net (Sample Number R1048-12) by ROV *ROPOS* directed by Anna Metaxas, 7 May 2007.

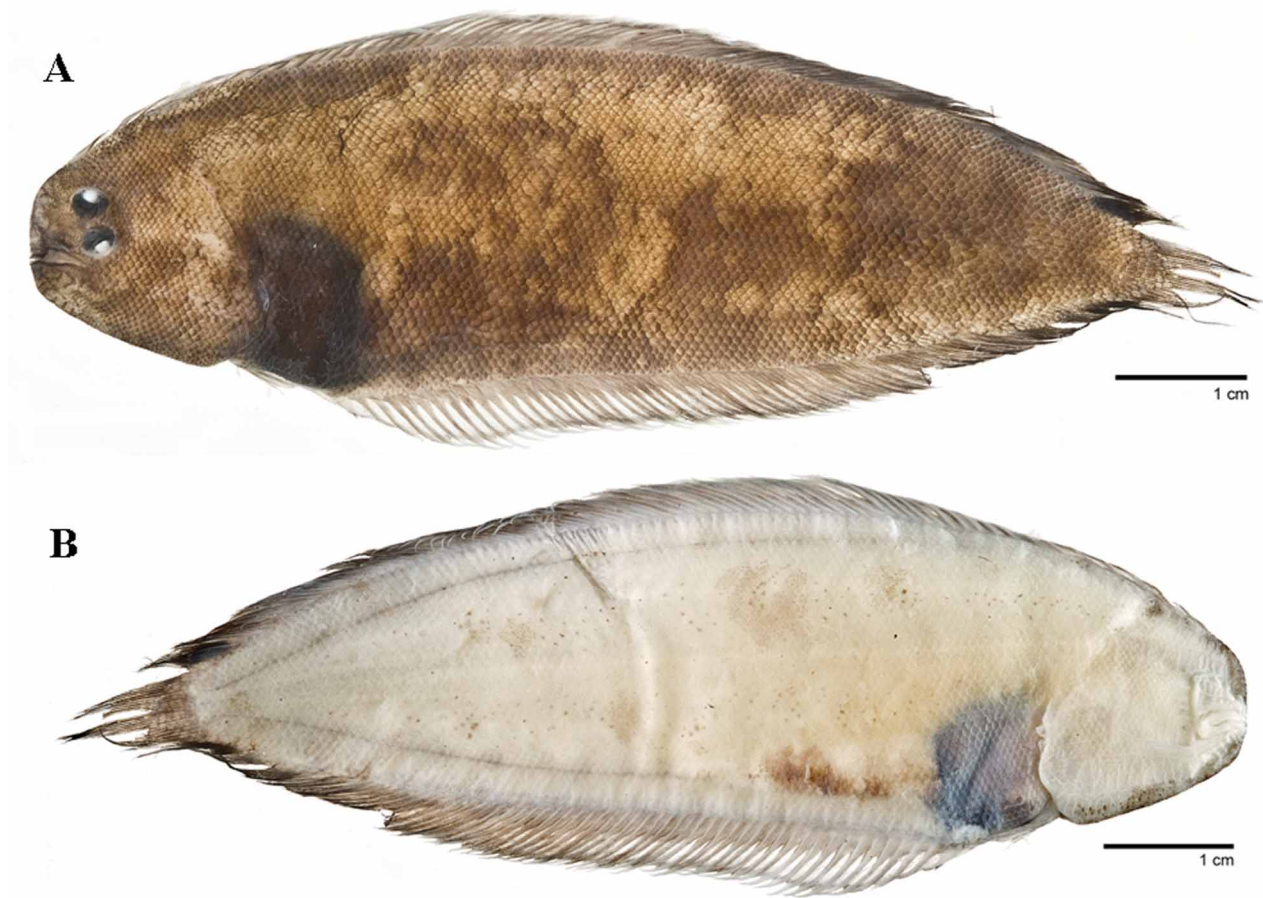


**FIGURE 2.** *Symphurus maculopinnis*, n. sp. (Holotype USNM 398820; female, 84.4 mm SL), collected at 561 m on Volcano-19, Tonga Arc, West Pacific. A. Ocular-side of alcohol-preserved specimen. B. Blind-side of same specimen.

**Diagnosis.** *Symphurus maculopinnis* is distinguished from all other species of *Symphurus* by the combination of a 1–2–2–2–1 ID pattern, 14 caudal-fin rays, 3+6 abdominal vertebrae, 49 total vertebrae, about 89 scales in a longitudinal row, 92 dorsal-fin rays, 77 anal-fin rays, a blunt squarish snout, blind-side lower jaw with thick lip with conspicuous plicae, and by conspicuous ocellated (sometimes partially) black spots on the posterior dorsal and anal fins.

**Description.** Morphological description based entirely on holotype (adult female, 84.4 mm SL; Figs. 1–5). A medium-sized species of *Symphurus* measuring to at least 100 mm SL [based on photographed specimens in Tunncliffe *et al.* (2010)]. ID pattern 1–2–2–2–1 (Figs. 3–4). Caudal-fin rays 14. Dorsal-fin rays 92. Anal-fin rays 76 (+1 fin ray missing). Pelvic-fin rays 4; posteriormost pelvic-ray connected to first anal-fin ray by delicate mem-

brane. Total vertebrae 49; abdominal vertebrae 9 (3+6) (Fig. 4). Hypurals 5. Longitudinal scale rows about 89. Scale rows on head posterior to lower orbit 21. Transverse scale rows 45.

Morphometrics (expressed as percentages of SL or HL; Table 1). Body moderately elongate (Fig. 2) with greatest body depth (29.6% SL) located in its anterior third (between anal-fin rays 10–25) and with gradual posterior taper. Preanal length slightly smaller than body depth. Head long, moderately wide, with squarish snout (Figs. 2A, 5); head length (21.6% SL) less than head width (25.6% SL; HW/HL = 1.20). Lower head lobe (12.7% SL) narrower than upper head lobe (16.2% SL); lower head lobe width less than postorbital length. Snout relatively broad with squarish anterior profile; snout length 18.1% HL; snout slightly longer than eye diameter. Dermal papillae conspicuously present on both ocular and blind sides of snout and head, but more numerous on blind-side head (Figs. 5A–B). Ocular-side snout and head with several short, vertical rows of dermal papillae as well as other

**TABLE 1.** Morphometric features for holotype (USNM 398820) of *Symphurus maculopinnis* n. sp. and 19 *S. ocellatus*. SL in mm; characters 2–9 in % of SL; 10–17 in % of HL.

Character	<i>S. maculopinnis</i> Holotype	<i>S. ocellatus</i> N=19
1. Standard length	84.4	75.6–120.5
2. Body depth	29.6	23.5–30.1
3. Preanal length	25.6	20.0–23.5
4. Head length	21.6	15.9–20.0
5. Head width	25.6	18.3–22.6
6. Postorbital length	13.5	10.5–13.7
7. Upper head lobe	16.2	9.9–15.6
8. Lower head lobe	12.7	7.4–11.9
9. Caudal-fin length	12.9	9.6–12.1
10. Postorbital length	62.6	63.0–68.5
11. Predorsal length	21.9	19.5–29.7
12. Snout length	18.1	15.6–21.7
13. Upper jaw length	25.8	20.3–24.8
14. Eye diameter	16.5	12.0–15.6
15. Chin depth	20.3	16.2–20.8
16. Upper opercular lobe	18.7	13.1–21.1
17. Lower opercular lobe	40.1	29.3–37.3
18. HW/HL	1.20	1.04–1.21
19. Pupil/Eye diameter	0.53	0.43–0.70

dermal papillae not arranged in obvious rows; ocular-side anterior head region dorsal to eyes with five, short, vertical rows of dermal papillae; anterior head region posterior to eyes with single, longer, horizontal row of dermal papillae; a single, short, vertical row of dermal papillae ventral to mid-region of lower eye; cheek region (ventral to lower jaw) with five, short, vertical rows of dermal papillae (Fig. 5A). Blind-side head and snout (Figs. 5B) with numerous, conspicuous, vertical and horizontal rows, sometimes interconnected, of dermal papillae extending nearly to ventro-posterior margin of opercle. Ocular-side anterior naris tubular, elongate; just reaching anterior margin of lower eye when depressed posteriorly. Posterior ocular-side naris a short, wide, tubular opening located nearly at vertical through anterior margin of pupil of lower eye. Blind-side anterior naris a short, slender, unpigmented tube located anterior to vertical through mid-jaw and barely perceptible among dense patch of dermal papillae. Blind-side posterior naris a short, posteriorly-directed tube located at posterior margin of dense patch of dermal papillae dorsal to horizontal through base of anterior blind-side nostril. Posterior margin of ocular-side maxilla at vertical through anterior region of pupil of lower eye. Ocular-side lower jaw without fleshy ridge. Blind-side lower jaw with thick lip with numerous plicae. Chin depth (20.3% HL) slightly greater than snout length (18.1% HL). Lower eye large (16.5% HL); eyes slightly subequal in position, anterior margin of lower eye at point

between verticals through anterior margin of upper eye and anterior margin of pupil of upper eye. Eyes separated by narrow interorbital space about 1–2 scales wide; dorsal aspects of eyes with 3–4 small, ctenoid scales; also with several rows of small ctenoid scales in interorbital space anteriorly. Pupillary operculum absent. Dorsal-fin origin at vertical through anterior margin of pupil of upper eye; predorsal distance 21.9% HL. Postorbital length 13.5% SL. Lower lobe of opercle (40.1% HL) twice as wide as upper opercular lobe (18.7% HL) and with its posterior margin extending noticeably further posteriorly than margin of upper opercular lobe.

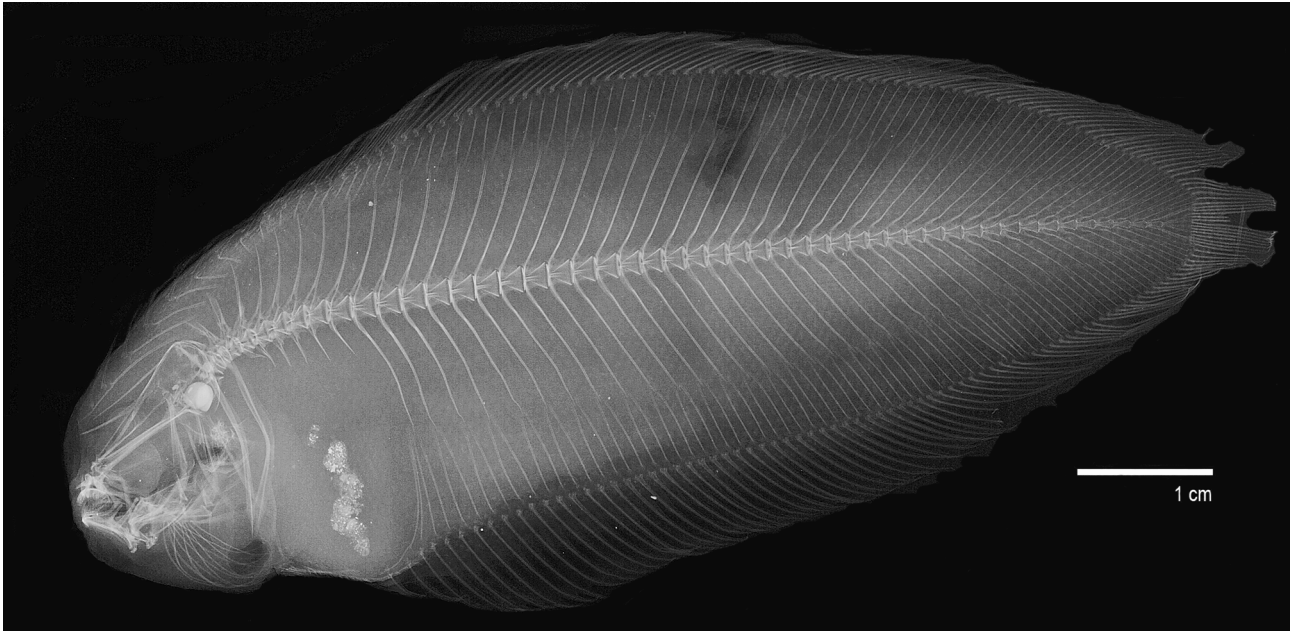


**FIGURE 3.** Radiograph of *Symphurus maculopinnis*, n. sp. (Holotype USNM 398820; female, 84.4 mm SL), collected at 561 m on Volcano-19, Tonga Arc, West Pacific.

Both sides of dorsal- and anal-fin rays without scales. Distal tips of most dorsal- and anal-fin rays free from interradiation membranes. Caudal fin short (12.9% SL), pointed, with middle fin rays slightly longer than others; basal halves on both sides of caudal fin with several rows of small, ctenoid scales.

Ocular-side dentary and maxilla with few teeth on their anterior regions. Blind-side dentary with 2–3 rows of well-developed teeth anteriorly expanding to several rows posteriorly; blind-side premaxilla with 2 rows of well-developed teeth curving slightly inwards.

Scales moderately large; ctenoid on both sides of body.

**Live color** (Figs. 1; 6–7; based on the holotype and other specimens photographed or videographed *in situ* at ~433–561 m on Volcano-19 from the ROV *ROPOS*; video edited by Jonathan Rose). Ocular-side head and body grayish-green to light brown and overlain with numerous, irregular, dark-brown blotches of various sizes; also with several incomplete, wide (5–7 scale rows), darker crossbands in midbody region and one complete crossband on caudal 1/4<sup>th</sup> of body; also with several smaller (2–4 scales wide), irregular white markings scattered over body surface, the largest of which overlies the dorsoanterior abdomen; and with two darker patches— one dorsal to pelvic fin on dorsoanterior abdomen and another situated at ventroposterior margin of abdomen.

Dorsal and anal fins each with a conspicuous, intense, ocellated (sometimes partially) black spot on their posteriormost rays (about the posteriormost 6–7 rays based on preserved specimen). Sometimes, black spots completely ocellated by white ring; otherwise, black spot only partially surrounded by one or two much smaller, irregular, white spots situated around its outer periphery. White pigment of dorsal-fin ocellus frequently not completely surrounding black spot near body nor as intense as ocellated ring and spots surrounding dark spot on anal fin. Dorsal and anal fins also with alternating series of lighter and darker blotches (about 4–6 fin-rays wide) throughout nearly entire length of fins. Dorsal-fin rays in anteriormost part of fin with distal thirds bright white and proximal two-thirds darker. Dorsal-fin rays in remainder of fin, and especially in more posterior blotches, more darkly pigmented over entire length of fin rays and also on fin membrane compared with those in blotches on anterior region of fin. Anal fin also with alternating series of lighter (some bright white) and darker blotches (about 4–

6 rays in each series) throughout length of fin to just before black spot on posteriormost fin rays. Anal-fin rays throughout entire fin pigmented over most of their lengths. Anteriormost anal-fin rays nearly entirely white, contrasting sharply to more heavily pigmented darker rays in remainder of fin. Anal-fin membrane in anterior region of fin pigmented only on its basal half, membrane in remainder of anal fin, especially that in dark blotches in posterior third of fin, more heavily pigmented nearly to its distal margin. Caudal fin dusky with several rays partially streaked with white and with several small whitish spots also on caudal-fin base. Pelvic-fin rays white throughout their lengths, in stark contrast to body color, especially contrasting against dark blotch on nearby abdomen.



**FIGURE 4.** Radiograph of head and anterior body region of Holotype (USNM 398820) of *Symphurus maculopinnis*, n. sp., depicting 1–2–2–2–1 pattern of interdigitation of anterior dorsal-fin pterygiophores and neural spines and nine abdominal vertebrae. Note also the sediment in the alimentary tract visible in this xray.

**Color in alcohol** (Figs. 2, 5; based only on holotype). Ocular-side background pigmentation uniformly medium dark brown with several diffuse, irregular, darker areas; region overlying abdomen dark, brownish-black (Fig. 2A). Ocular-side head and body scales with posterior halves of exposed region more darkly pigmented than anterior halves of exposed portions. Head coloration similar to that on body, except posterior margin of opercle outlined in black (Fig. 5A). Snout nearly to distal tip with similar pigment as that on rest of head; distalmost snout

region lighter than more posterior regions. Ocular-side lips dark black, except posteriormost parts of upper and lower lips lighter brown. Ocular-side anterior nostril black for most of its length; distalmost tip whitish. Ocular-side inner opercular lining white, ventral half with several faint melanophores; inner lining of blind-side opercle white. Isthmus on both sides with small melanophores, more concentrated on ocular-side isthmus than on blind-side counterpart.

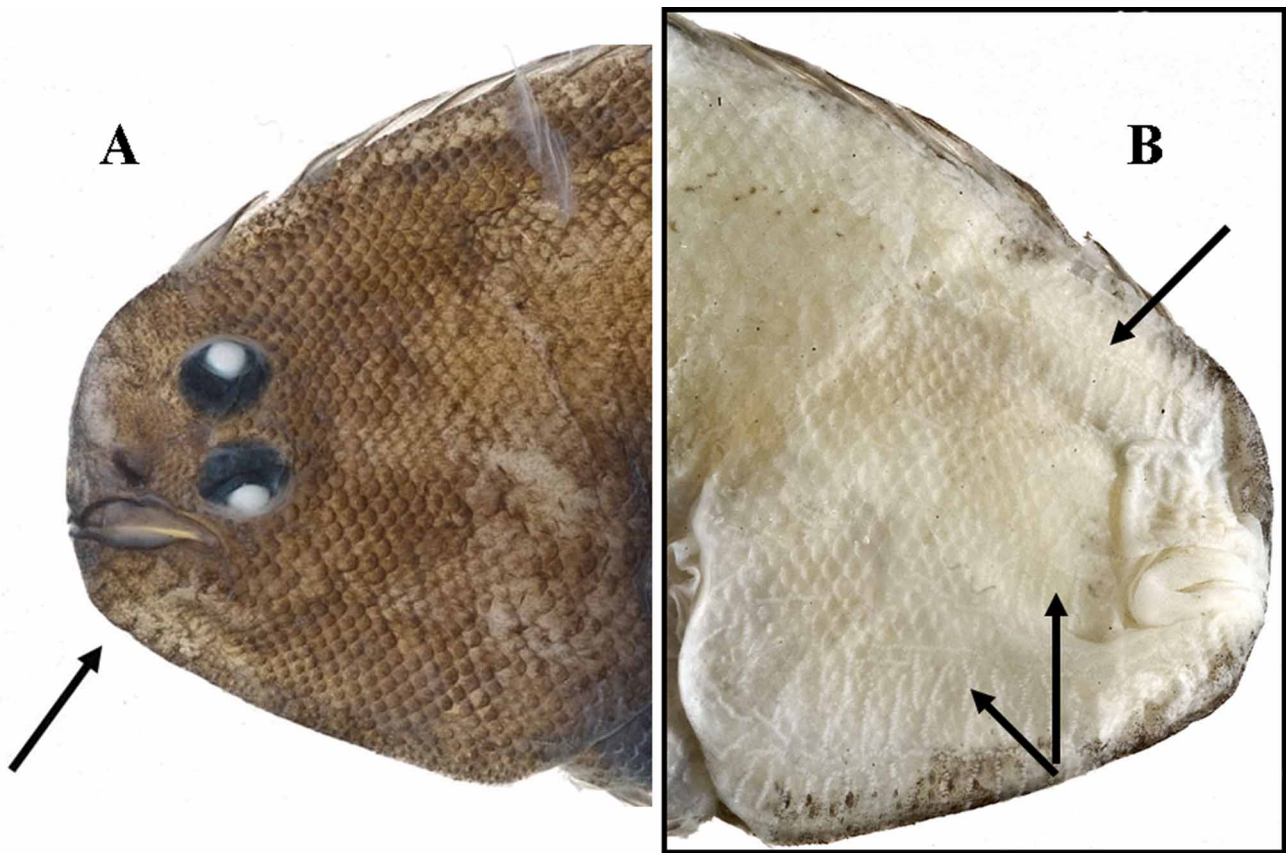


**FIGURE 5.** Close-up views of ocular (A) and blind (B) sides of head of *Symphurus maculopinnis*, n. sp. (Holotype USNM 398820; female, 84.4 mm SL) collected at 561 m on Volcano-19, Tonga Arc, West Pacific. Arrows indicate areas with conspicuous rows of dermal papillae.

Blind-side background coloration of head and body uniformly whitish except for dark, bluish-black abdomen (Figs. 2B, 5B). Dorsal and ventral margins of blind-side head (Fig. 5B) also with numerous, small, darkly-pigmented melanophores on several rows of scales (similar in color to scales on ocular-side head); central portion of posterior region of blind-side head with irregular patch of numerous, faint, small melanophores (visible under magnification). Two nearly parallel, zig-zagging rows of clusters of faintly-pigmented melanophores extending posteriorly from posterior margin of head nearly to caudal-fin base (Fig. 2B); dorsal row located about 1/4<sup>th</sup> body width from dorsal-fin base, ventral row located medially just ventral to body mid-point. Single row of faint melanophores evident internally in dermis about at medial ends of proximal pterygiophores in both posterior 3/4ths of dorsal fin and for nearly entire length of anal fin. Ventroanterior region of blind-side abdomen dorsal to pelvic fin with dark patch of scales. Anal sphincter white. Blind-side body also with short, diffuse, continuous, dark sooty-brown smudge located dorsal to anal-fin rays 6–17 (corresponding to location of ovary).

Ocular sides of dorsal and anal fins uniformly sooty-gray throughout most of their lengths. Most fin rays streaked with darker pigment than that on connecting membranes, distalmost tips of fin rays white (Fig. 2A). Pigment on rays and membranes progressively intensifying posteriorly in both fins. Dorsal and anal fins also with single, conspicuous, non-ocellated, black spot on their posteriormost rays. Anteriormost dorsal-fin rays streaked with dark pigment contrasting with lightly pigmented connecting membranes. Next several successive dorsal-fin rays also more darkly pigmented than connecting membranes, but membranes also feature clusters of melanophores in their distal sections. At about 1/3 length of fin and continuing posteriorly, nearly entire dorsal-fin membrane cov-

ered with darker melanophores. Posteriormost six dorsal-fin rays with conspicuous black spot extending from fin base (and also slightly on body) to nearly distalmost tips of rays.

Blind sides of anteriormost 3–4 dorsal-fin rays with speckling along entire lengths of rays and also on connecting membranes (Fig. 2B). Successive rays in anterior fin generally whitish with faint, small melanophores on rays and membrane. Pigmentation similar throughout remainder of fin, but becoming progressively darker posteriorly, and culminating with posteriormost rays bearing dark spot.

Ocular sides of anteriormost anal-fin rays more lightly streaked than those of more posterior rays; their connecting membranes only lightly pigmented in their distal regions. At about midpoint of anal fin, pigment covers entire interradiation membrane. Seven posteriormost anal-fin rays covered by intense black spot extending from fin-ray bases nearly to distalmost tips.

Blind side of anal fin generally whitish anteriorly, with rays in anterior one-third of fin with faint melanophores; pigmentation progressively intensifying posteriorly, with darkest pigment on posteriormost fin rays bearing spot.

Ocular sides of pelvic-fin rays with dark melanophores similar to those on anal fin; blind side of pelvic fin whitish, with faint, small, darker spots. Both sides of caudal fin uniformly sooty grayish-black throughout; ocular side of fin darker than blind side. Both sides of caudal fin with nearly entire lengths of rays and their connecting membranes heavily pigmented, and with distal thirds of central caudal-fin rays darker (nearly black) compared with their proximal two-thirds. Small, ctenoid scales on basal half of both sides of caudal fin with numerous, small, darkly-pigmented melanophores scattered over their exposed surfaces (best viewed under magnification).

**Distribution and habitat.** *Symphurus maculopinnis* is known only from the holotype, collected on soft sediments at 561 m (Fig. 1), and 56 other individuals observed, but not collected, on a variety of substrata, including coarse gravel, gravelly sand-shell and gravelly sand (Figs. 6–7), located between 433–561 m on Volcano-19, Tonga Arc, western Pacific. Tunnicliffe *et al.* (2010: Table 2) indicated that this species was also observed at shallower depths (between 195–381 m) at a second, nearby site (Volcano-1). However, re-examination of photographs indicates that the individuals upon which these observations were based can not be positively identified. Thus, reported occurrences of *S. maculopinnis* both at Volcano-1 and at these shallower depths is tenuous.

*Symphurus maculopinnis* is considered to be a true vent species (Tunnicliffe *et al.* 2010) as it was most often observed (90% of 57 observations) within 30 m of point sources of obvious venting. It was observed to be abundant in areas near a high temperature vent that also supported abundant clams in the surrounding sediments. A probe inserted ca. 10 cm in the sediments registered 11°C (bottom water temperature 5°C), which indicated an area of low flux of hydrothermal fluid. *Symphurus maculopinnis* was not observed at other vent sites located deeper than 600 m either on Volcano-19 or at other volcanoes studied by Tunnicliffe *et al.* (2010).

**Etymology.** The specific name, *maculopinnis*, from the Latin *macula*, meaning spot, and *pinna*, meaning fin, in reference to the conspicuous spots on the dorsal and anal fins of this species. To be treated as a noun in apposition.

**Remarks.** The holotype of *S. maculopinnis*, the only specimen collected and radiographed thus far (Figs. 3–4), features 14 caudal-fin rays, 9 abdominal vertebrae and a 1–2–2–2–1 ID pattern (Fig. 4). The 1–2–2–2–1 ID pattern is unusual among symphurine tonguefishes (Munroe 1992) as none of the 79+ nominal species of *Symphurus* examined to date feature a predominant 1–2–2–2–1 ID pattern (Munroe 1992; Munroe unpubl. data; Lee *et al.* 2009a; 2009b). Most species in the genus that have 14 caudal-fin rays and 9 abdominal vertebrae (N= 19 species) have either the 1–2–2–2–2 (14 species) or the 1–2–3–2–2 ID pattern (3 species) as their predominant pattern (Munroe 1992; Krabbenhoft & Munroe 2003; Munroe 2006; Munroe & Hashimoto 2008; Lee *et al.* 2009a, 2009b). Another seven species in the genus, also with 14 caudal-fin rays, have an ID pattern similar to that observed in the holotype of *S. maculopinnis*, where only a single pterygiophore inserts into interneural space 4 (1–2–2–1–2 ID pattern). However, four of these species also have 10 abdominal vertebrae (compared with only nine in *S. maculopinnis*). Number of abdominal vertebrae, a very conservative character within *Symphurus*, is one of the most reliable meristic characters useful in diagnosing these species. Three other species, *S. fuscus* Brauer, *S. macrophthalmus* Norman and *S. schultzi* Chabanaud, have 9 abdominal vertebrae and 14 caudal-fin rays (Munroe 1992) and, based on the limited data available for these species, also appear to have an ID pattern featuring a 1–2–2–1–2 arrangement of pterygiophores, which is similar to that observed in *S. maculopinnis*. All three species have been rarely captured and the data are insufficient to determine whether this is their predominant ID pattern. The ID pattern of

*S. fuscus*, for example, is known only from the holotype; that of *S. macrophthalmus* is known from the holotype and a paratype; and for *S. schultzi*, two patterns are represented among four paratypes (all with 1–2–2–1–2 ID pattern) and the holotype (with 1–2–2–2–2 ID pattern).

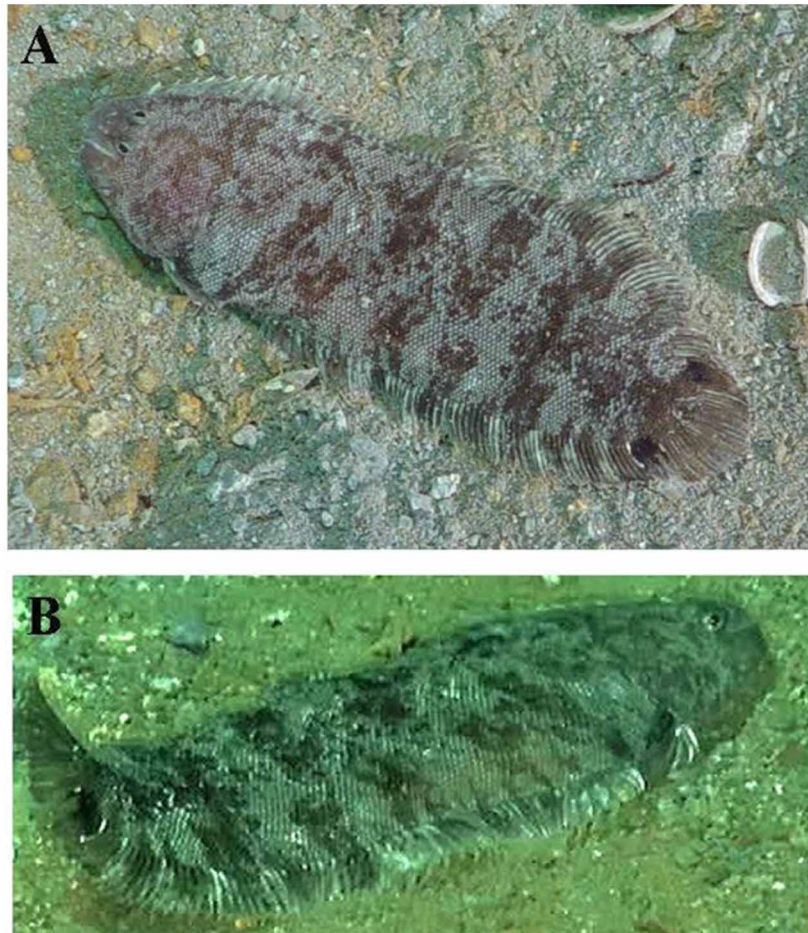


**FIGURE 6.** *In situ* photographs of two individuals of *Symphurus maculopinnis*, **n. sp.**, observed on Volcano–19, Tonga Arc, West Pacific, featuring different asymmetries. A. Specimen with sinistral asymmetry photographed at ca. 439 m. B. Frame grab of specimen featuring reversed (dextral) asymmetry videographed at ca. 560 m. Note also posture of both fish with raised caudal regions displaying prominent spots on posterior dorsal and anal fins as they swim over the bottom.

Although the ID pattern of the holotype of *S. maculopinnis* features only a single pterygiophore inserted into the fifth interneural space, it is possible that this is not the predominant ID pattern for this species. More likely, the predominant ID formula for this species is 1–2–2–2–2. Among 14 species characterized by the 1–2–2–2–2 ID pattern, some individuals are observed, albeit infrequently, with a variant 1–2–2–2–1 ID pattern (6 of 258 individuals or 2.3% of specimens radiographed). Alternatively, if the predominant ID pattern for *S. maculopinnis* is found to be 1–2–2–2–1, then, based on what is presently known about ID patterns in symphurine tonguefishes, this species would feature a unique predominant ID pattern among species of *Symphurus*. Determination of the predominant ID pattern for *S. maculopinnis*, as for several other deepwater symphurine species, will have to await collection of additional specimens.

*Symphurus maculopinnis* is the third tonguefish species known to inhabit hydrothermal vent areas, all of which are located on western Pacific Ocean volcanic arcs (Tunnicliffe *et al.* 2010). Other species found at hydrothermal vents include *S. thermophilus* (Munroe & Hashimoto, 2008), and undescribed “species A” recently discovered by Tunnicliffe *et al.* (2010). Munroe and Hashimoto (2008) described *S. thermophilus*, based on specimens collected at hydrothermal sites located in the North Pacific and South Pacific oceans. However, analysis of mitochondrial DNA samples and morphological comparisons (Tunnicliffe *et al.* 2010) reveal that two species are represented among specimens previously identified as *S. thermophilus*. Based on their results, Tunnicliffe *et al.* (2010) deter-

mined that *S. thermophilus* is known at hydrothermal sites only in the northwest Pacific Ocean, while undescribed species A (including some specimens previously identified as *S. thermophilus* by Munroe & Hashimoto) occurs in the South Pacific Ocean on several volcanoes along the Kermadec–Tonga Arc between New Zealand and Samoa.

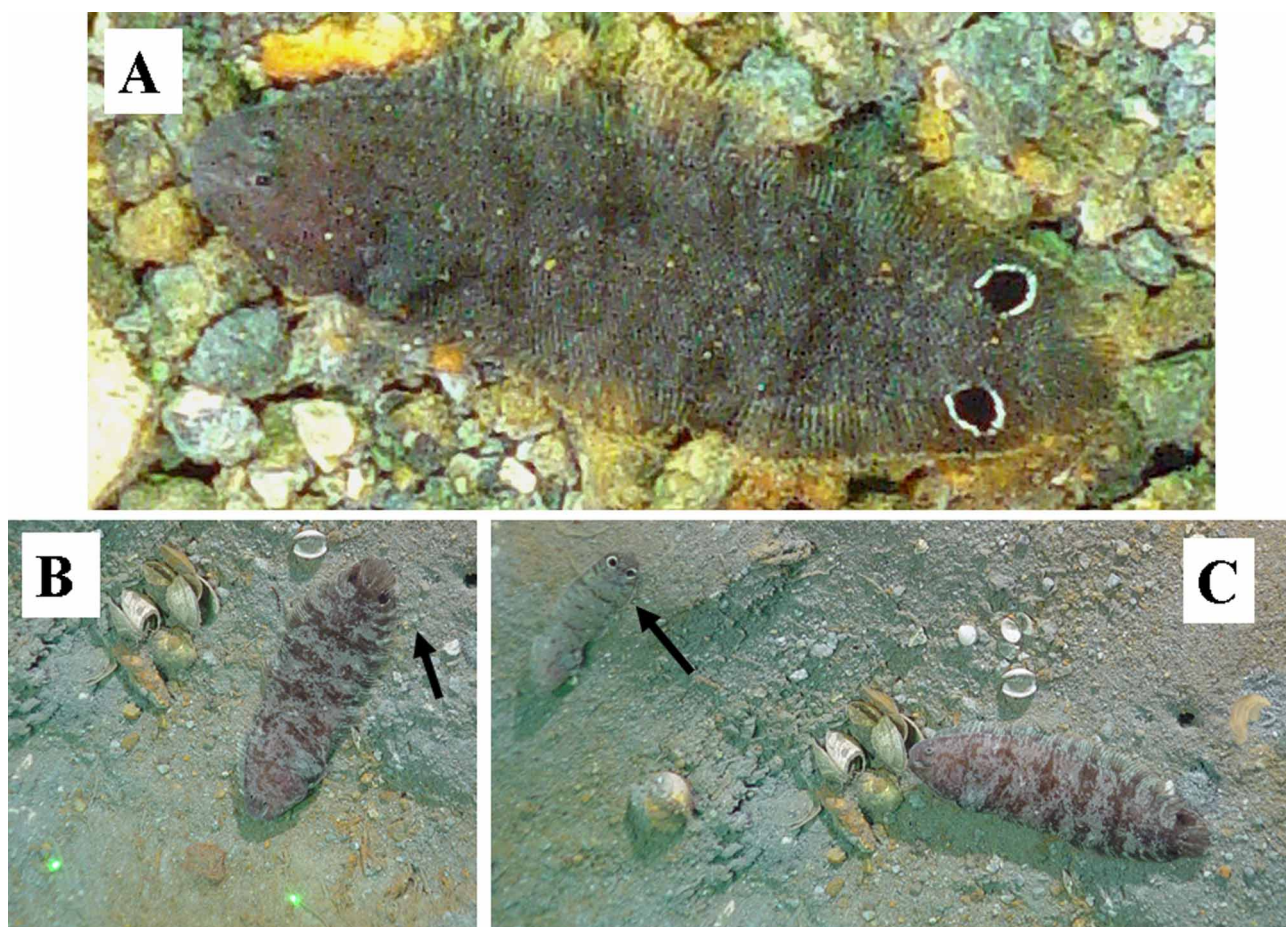


**FIGURE 7.** *In situ* photographs of three individuals of *Symphurus maculopinnis*, n. sp. observed on Volcano-19, Tonga Arc, West Pacific, illustrating variation in live coloration, variety of substrata inhabited by this species, and interesting posture of raising the caudal region (indicated by arrows) thereby displaying prominent spots on the posterior dorsal and anal fins. A. Specimen with conspicuous, complete ocellus on dorsal and anal fins photographed on coarse pebbly substratum. B. Specimen (ca. 12.4 cm in length based on 10 cm distance between green laser dots) with incomplete white ring around black fin spots photographed on gravelly sand-shell substratum. C. Two specimens photographed on gravelly sand-shell substratum. Smaller specimen features complete ocellus on dorsal and anal fins and slight banding on body; larger specimen features little, if any, white pigment around periphery of black fin spots and distinct banding on body.

At least 10 of the 79+ described species of *Symphurus*, including *S. maculopinnis*, have prominent (sometimes ocellated) spots on their dorsal, anal or caudal fins. These species live at a variety of depths ranging from 4 to 640 m (most occur in < 100 m) and inhabit environments from white, sandy substrata in shallow seagrass beds in clear tropical waters to various substrata in relatively dim lit waters on the upper continental slope and at seamounts. Of species with ocellated fins, only three occupy relatively deepwater habitats; *S. stigmosus* Munroe occurs from 192–373 m (Munroe 1998), *S. ocellatus* occurs from 430–640 m (Munroe, unpub. data), and *S. maculopinnis* occurs between 433–561 m (Tunnicliffe *et al.* 2011). None of the deepest-dwelling (800–1500 m) species of *Symphurus* have ocellated fins. In a detailed study (1200 specimens, 50 species) of the occurrence of ocellated spots on dorsal fins in the deepsea ophiidiid genus *Neobythites* Goode & Bean, Uiblein & Nielsen (2005) report 22 of 50 species in this genus with distinct ocelli and that these species occur at mean collecting depths ranging from 150 to 450 m, depths not all that different than those recorded for the three deepest-dwelling species of *Symphurus* with ocellated fins.

Since a lower depth limit for color vision in clear oceanic waters is estimated to occur at about 550 m (Clarke & Denton 1961), the deeper depths where some of these species of *Symphurus* and *Neobythites* (Uiblein & Nielsen

2005) with ocellated fins occur may have natural light levels that are low to non-existent. Detection of visual signals, such as ocellated spots, in depths where light levels are low might appear to be limited in species inhabiting such depths and their usefulness as signals questionable. However, Uiblein & Nielsen (2005) cited several studies among shallow-water fishes living in reduced light conditions where visual acuity is low that provide evidence these species may effectively use contrasting body coloration for signaling. Uiblein & Nielsen (2005) note further that ocelli are among the most contrasting color patterns and hence should be visible in semidark habitats such as those on the lower continental shelf and upper continental slope. This would apply equally well on Volcano-19 where the depths occupied by *S. maculopinnis* are in similar low-light environments.

No behavioral observations have been made on tonguefishes with ocellated fins regarding the function of such conspicuous pigmentation features. For other fishes, ocellated pigment spots have been suggested to serve as species recognition signals (Kohda & Watanabe 1990; Uiblein & Nielsen 2005) or as antipredator devices (Neudecker 1989; Hasson 1991; Uiblein & Nielsen 2005). During the course of exploration of hydrothermal vent areas and other habitats on Volcano-19, 57 individuals of *S. maculopinnis* occurred in ROV imagery (Tunnicliffe *et al.* 2010). Examination of the behavior of these tonguefishes provides some insight into the function of ocellated fin spots in this species. Tunnicliffe *et al.* (2010) note that individuals of *S. maculopinnis* appeared to be more quiescent than representatives of *Symphurus* species A observed in the same areas. Individual *S. maculopinnis* were observed to flip sediment over their bodies to increase their camouflage, and when approached by another fish, one *S. maculopinnis* raised its tail, thereby elevating the conspicuous eyespots on the dorsal and anal fins. We note two other videographed individuals of *S. maculopinnis* closely associated with the coarse sedimentary substratum that were initially at rest and partially buried (video available at <http://ocean.si.edu/ocean-videos/tonguefish-underwater-volcano-19>). They then began to swim slowly over the substratum propelled by flexing anterior to posterior waves of muscle contraction down the body and dorsal and anal fins. While swimming, these two fish also exhibited a similar posture of raised posterior body regions with dorsal- and anal-fin rays widely spread thereby conspicuously displaying the pigmented spots on these fins. Several other individuals observed and photographed on the seamount also had raised caudal regions displaying their prominent ocellated fins (see Figs. 6A–B; 7B–C). Numerous observations of individuals of *S. maculopinnis* displaying a swimming posture with eyespots prominently displayed when in the presence of conspecifics suggests that this posture serves as a species recognition signal among conspecifics.

It is also possible that having eyespots so prominently displayed on up-raised and expanded fins also increases the appearance of these tonguefishes beyond their actual size, whereby these ocellated spots would then function as an antipredator mechanism. An enlarged appearance may deter visually hunting predators (Hasson 1991), or possibly, as is the case with these tonguefishes with spots located on their posterior fins, the spots may confuse a predator into attacking the posterior end of the potential prey's body where a vital zone is less likely to be struck (Neudecker 1989; Hasson 1991), or where the attack zone may even allow the tonguefish to escape altogether as it darts forward away from the predator's point of attack at the rear of its body. Little is known about potential predators or predation rates on tonguefishes at hydrothermal vent areas (or elsewhere) and these aspects of their ecology remain areas in need of further study.

Among videographed *S. maculopinnis* was a specimen featuring reversed (dextral) asymmetry (see Fig. 6B). Based on observations from the short video of this specimen, it appears to be indistinguishable both in its morphology, save for its reversed asymmetry, and its behavior from the other, non-reversed specimens of *S. maculopinnis* appearing in this and other videos (Figs. 6A, 7A–C).

Capture of deepwater (>200 m) tonguefish with reversed asymmetry is rare, as only one other specimen, that of the eastern Atlantic *S. vanmelleae* Chabanaud, is known (Munroe 1996). This video sequence of a reversed *S. maculopinnis* is also the first to observe behavior of a reversed individual of *Symphurus*, and represents the first sequence to record *in situ* the reactions of conspecifics to behavior and movements of another conspecific with reversed asymmetry.

**Comparisons.** *Symphurus maculopinnis* is only the second known Indo–West Pacific species of *Symphurus* characterized by the combination of 14 caudal-fin rays, a 1–2–2–2–2 ID pattern (assuming this is predominant pattern for the species; see Remarks Section above), and pigmented spots on its dorsal and anal fins. The only other species of *Symphurus* featuring this combination of characters is *S. ocellatus*, known from deep waters (430–640 m) off East Africa (Heemstra 1986). *Symphurus maculopinnis* differs from *S. ocellatus* in having lower, and non-overlapping, meristic features (total vertebrae 49 vs. 54–56, dorsal-fin rays 92 vs. 97–103, anal-fin rays 77 vs. 85–

89), a blunt, squarish snout (vs. more pointed snout), thick blind-side lower lip with conspicuous plicae (vs. thin blind-side lip without conspicuous plicae), longer (21.6% SL vs. 15.9–20.0% SL) and wider head (head width 25.6% SL vs. 18.3–22.6), and wider upper (16.2% SL vs. 9.9–15.6% SL) and lower (12.7% SL vs. 7.4–11.9% SL) in *S. ocellatus*) head lobes.

Other species of *Symphurus* with 14 caudal-fin rays and 50 or fewer total vertebrae include *S. macrophthalmus*, *S. schultzi*, *S. monostigmus* Munroe, *S. bathyspilus* Krabbenhoft and Munroe, *S. multimaculatus* Lee *et al.*, and two other species that occur at hydrothermal vent areas, *S. thermophilus* and undescribed Species A, which is closely related to *S. thermophilus* (Tunncliffe *et al.* 2010). *Symphurus maculopinnis* differs from all of these other species in having spots on the dorsal and anal fins. *Symphurus maculopinnis* differs further from *S. macrophthalmus*, a rarely-captured species known only from the holotype and a paratype (in pieces) collected between 457–549 m in the Gulf of Aden (Norman 1939), in having a smaller eye diameter (ED) (ED 16.5% HL vs. 21.1% HL in *S. macrophthalmus*).

*Symphurus maculopinnis* differs further from *S. monostigmus*, known from two specimens collected in relatively shallow waters (65–100 m) off East Africa (Munroe 2006), in having a darkly-pigmented ocular side with conspicuous dark blotches and incomplete crossbands (vs. ocular side lightly pigmented with numerous freckles in *S. monostigmus*). *Symphurus maculopinnis* also has a larger pupil (pupil diameter/eye diameter = 53% compared with that of *S. monostigmus* (28–32%), a longer, narrower head (HW/HL = 1.20 vs. 1.39–1.42), a shorter postorbital length (POL) relative to head length (POL/HL = 62.6% vs. 75.5–80.5%), a longer snout (18.1% HL vs. 14.5–17.2% HL) and larger eye (ED = 16.5% HL vs. 10.0–13.8% HL), several small scales in the interorbital space and on upper aspects of the eyes (scales absent in these areas in *S. monostigmus*), and *S. maculopinnis* has a wider lower opercular lobe compared with the upper opercular lobe (vs. upper opercular lobe wider than lower opercular lobe in *S. monostigmus*).

*Symphurus maculopinnis* differs from *S. bathyspilus*, a deepwater (248–500 m) species occurring in the Philippine Archipelago and Indonesia (Krabbenhoft & Munroe 2003), in its squarish anterior head profile (vs. longer, pointed snout profile) and different blind-side pigmentation (white with relatively few melanophores arranged in zig-zag longitudinal rows vs. blind-side white with numerous melanophores scattered over blind-side surface and heavier covering of melanophores primarily over pterygiophore regions of dorsal and anal fins). *Symphurus maculopinnis* may have fewer dorsal- and anal-fin rays than does *S. bathyspilus*, as counts for these features in the holotype only overlap the lower end of ranges of these meristic features in *S. bathyspilus*. Additionally, the holotype of *S. maculopinnis* has 49 total vertebrae and 45 scales in a transverse row versus the 50–54, usually 51–52, total vertebrae and 29–34 scales in a transverse row in *S. bathyspilus*. Several morphometrics of the holotype also differ from those of *S. bathyspilus* including its deeper body (body depth 29.6% SL vs. 21.8–25.8% SL), a smaller POL (62.6% HL vs. 63.6–71.6% HL), and a wider upper head lobe (16.2% HL vs. 8.9–13.0% HL). The dorsal-fin origin (anterior margin of pupil of upper eye) is located more anteriorly on the holotype of *S. maculopinnis* than is that of *S. bathyspilus* (located between verticals through middle and posterior margin of upper eye).

Most meristic and morphometric features of *S. maculopinnis* overlap those of *S. schultzi*, a deepwater species collected between 479–1013 m in the Philippine Archipelago (Chabanaud 1955), which is known only from four paratypes (all with 1–2–2–1–2 ID pattern) and the holotype (with 1–2–2–2–2 pattern). The holotype of *S. maculopinnis* differs in having 89 scales in a longitudinal series compared with 70–80 longitudinal scales in *S. schultzi*. The two species also differ in the anterior profile of the head (squarish in *S. maculopinnis* vs. more pointed in *S. schultzi*). The color patterns of the two species are also different. Chabanaud (1955) indicated the type series of *S. schultzi* featured an evenly pigmented reddish-brown ocular side (specimens now faded), which is distinctly different from that observed in the holotype and other specimens videographed of *S. maculopinnis*.

*Symphurus maculopinnis* has similar meristic features to those of *S. multimaculatus* Lee *et al.* collected in deep waters (exact depths unknown, but thought to occur deeper than 300 m) off Taiwan (Lee *et al.* 2009a), but differs distinctly from this species in its squarish anterior profile (vs. pointed anterior profile) and more elongate body with greatest depth occurring over larger part of mid-body with gradual anterior and posterior taper (vs. greatest body depth occurring over shorter part of mid-body with rapid anterior taper in *S. multimaculatus*). The two species also differ in aspects of their blind-side coloration including the white opercle with few melanophores in *S. maculopinnis* (vs. bluish-black blind-side opercle in *S. multimaculatus*) and the blind-side body mostly white with zig-zag arrangement of melanophores (vs. blind side with dense concentrations of blackish-brown melanophores predominately covering pterygiophore regions of dorsal and anal fins). *Symphurus maculopinnis* has fewer longitudi-

nal and transverse scale rows (89 vs. 102–108, and 45 vs. 50–51) than does *S. multimaculatus*. Differences in the morphology of these species are also evident in: ratios of head width to head length (HW/HL 1.20 vs. 1.26–1.50, reflecting that *S. maculopinnis* has a shorter and narrower head); in eye diameters (16.5% HL in *S. maculopinnis* vs. 9.1–10.1% HL); postorbital head lengths (shorter in *S. maculopinnis* 62.6% HL vs. 67.8–71.7% HL in *S. multimaculatus*); and pupil size (pupil diameter 53% of eye diameter in *S. maculopinnis* vs. 61–72% in *S. multimaculatus*).

The two other tonguefishes captured at western Pacific hydrothermal vents, *S. thermophilus* (Munroe & Hashimoto 2008) and the closely-related and undescribed *Symphurus* Species A of Tunnicliffe *et al.* (2010) from the Kermadec Ridge, also have 14 caudal-fin rays, similar ID patterns, and overlapping counts for total vertebrae and dorsal- and anal-fin rays with those observed in *S. maculopinnis*. Neither species has spots on the dorsal and anal fins so they can readily be distinguished from *S. maculopinnis* as long as pigment is present on fins of the specimens. *Symphurus maculopinnis* differs further from both species in its more elongate body with gradual taper (vs. greatest body depth in anterior third of body with more rapid posterior taper), in having larger scales (89 in longitudinal series vs. 100–112), a larger lower opercular lobe (40.1% HL vs. 26.9–36.4% HL), smaller upper opercular lobe (18.7% HL vs. 21.7–36.4% HL), and shorter predorsal length (21.9% HL vs. 24.2–31.9% HL in these others). Additionally, genetic data also support the hypothesis that *S. maculopinnis* differs distinctly from these other species as Tunnicliffe *et al.* (2010) found a genetic distance of 30% (COI) and 14% (16s rRNA) between *S. maculopinnis* and *S. thermophilus/Symphurus* species A.

## Acknowledgments

L. Willis provided radiographs of the holotype and L. Willis and M. Nizinski provided radiographs of specimens used in the comparisons. J. Clayton and D. Smith assisted with accessioning and cataloguing the holotype. J. Rose compiled the videotape of specimens filmed *in situ* at Volcano-19 and provided field data associated with the holotype; C. Marzec and M. Benson assisted with publishing and archiving the tonguefish video to the Smithsonian Institution's Ocean Portal website; C. Ames assisted with making video grabs from video tapes. S. Raredon provided photographs of the holotype. Appreciation is extended to curators and collection staff who provided assistance locating specimens, providing catalogue information, or who arranged for loan of specimens used in this study. We acknowledge the field team who collected and filmed this species during the SO192–2 MANGO Expedition, particularly S. K. Juniper and C. Stevens; expedition co-chiefs were U. Schwarz-Schampera and M. Hannington with R/V *Sonne* and ROV *ROPOS*. Collection of this specimen was made possible by funding provided to V. Tunnicliffe by NSERC Canada.

## Literature cited

- Chabanaud, P. (1955) Flatfishes of the genus *Symphurus* from the U.S.S. "Albatross" Expedition to the Philippines, 1907–1910, *Journal of the Washington Academy of Sciences*, 45(1), 30–32.
- Clarke, G.L., & Denton, E.J. (1961) Light and Animal Life. In: Hill, M.N. (ed.), *The Sea*. Wiley, New York, pp. 456–468.
- Hasson, O. (1991) Pursuit-deterrent signals: communication between prey and predator. *Trends in Ecology and Evolution*, 6, 325–329.
- Heemstra, P.C. (1986) Family Cynoglossidae. In: Smith, M.M., & Heemstra, P.C. (Eds.), *Smith's Sea Fishes*, 1<sup>st</sup> ed. Southern Book Publishers, Johannesburg, pp. 865–868.
- Kohda, Y., & Watanabe, M. (1990) The aggression-releasing effect of the eye-like spot of the oyanirami *Coreoperca kawamabari*, a freshwater serranid fish, *Ethology*, 84, 162–166.
- Krabbenhoft, T.J., & Munroe, T.A. (2003) *Symphurus bathyspilus*: a new cynoglossid flatfish (Pleuronectiformes: Cynoglossidae) from deepwaters of the Indo–West Pacific, *Copeia*, 2003(4), 810–817.
- Lee, M.-Y., Munroe, T.A., & Chen, H.-M. (2009a) A new species of tonguefish (Pleuronectiformes: Cynoglossidae) from Taiwanese waters, *Zootaxa*, 2203, 49–58.
- Lee, M.-Y., Shao, K.-T., & Chen, H.-M. (2009b) A new species of deep-water tonguefish Genus *Symphurus* (Pleuronectiformes: Cynoglossidae) from Taiwan, *Copeia*, 2009(2), 342–347.
- Munroe, T.A. (1992) Interdigitation pattern of dorsal-fin pterygiophores and neural spines, an important diagnostic character for symphurine tonguefishes (*Symphurus*: Cynoglossidae: Pleuronectiformes), *Bulletin of Marine Science*, 50(3), 357–403.

- Munroe, T.A. (1996) First record of reversal in *Symphurus vanmelleae* (Pleuronectiformes: Cynoglossidae), a deep-water tonguefish from the tropical eastern Atlantic, *Cybium*, 20(1), 47–53.
- Munroe, T.A. (1998) Systematics and ecology of tonguefishes of the genus *Symphurus* (Cynoglossidae: Pleuronectiformes) from the western Atlantic Ocean, *Fishery Bulletin*, 96(1), 1–182.
- Munroe, T.A. (2006) New western Indian Ocean tonguefish (Pleuronectiformes: Cynoglossidae, *Symphurus*), *Copeia*, 2006(2), 230–234.
- Munroe, T.A., & Hashimoto, J. (2008) A new western Pacific tonguefish (Pleuronectiformes: Cynoglossidae): The first pleuronectiform discovered at active hydrothermal vents, *Zootaxa*, 1839, 43–59.
- Neudecker, S. (1989) Eye camouflage and false eyespots: chaetodontid responses to predators, *Environmental Biology of Fishes*, 25, 143–157.
- Norman, J.R. (1939) Fishes. The John Murray Expedition. 1933–34. *Scientific Reports of the John Murray Expedition*, 7, 1–116.
- Stoffers, P., Worthington, T.J., Schwarz-Schampera, U., Hannington, M.D., Massoth, G.J., Hekinian, R., Schmidt, M., Lundsten, L.J., Evans, L.J., Vaiomo'unga, R., & Kerby, T. (2006) Submarine volcanoes and high-temperature hydrothermal venting on the Tonga arc, southwest Pacific, *Geology*, 34, 453–456.
- Tunncliffe, V., Koop, B.F., Tyler, J., & So, S. (2010) Flatfish at seamount hydrothermal vents show strong genetic divergence between volcanic arcs, *Marine Ecology*, 31(Suppl. 1), 1–9.
- Uiblein, F., & Nielsen, J.G. (2005) Ocellus variation and possible functions in the genus *Neobythites* (Teleostei: Ophidiidae), *Ichthyological Research*, 52, 364–372.